Accounting for Parameter Uncertainties in Model Verification: An Illustration with Tropical Sea Surface Temperature*

M. BENNO BLUMENTHAL AND MARK A. CANE

Lamont-Doherty Geological Observatory of Columbia University, Palisades, New York

(Manuscript received 6 May 1988, in final form 17 January 1989)

ABSTRACT

A simplified model originally developed to simulate sea surface temperature (SST) in the tropical Pacific is extended in two directions. First, the model is formulated and run for the tropical Atlantic. Second, optimal values are determined for a number of model parameters, especially those determining surface heat flux. In the Pacific, the difference between model SST and data SST is the size of the probable error due to uncertainties in the heat flux, O (35 W m^{-2}). In the equatorial Atlantic the discrepancies may also be attributed to heat flux errors, but model–data differences in the Atlantic near coastal regions north of 10°N and south of 10°S are too large to be explained by heat flux errors: model problems involving other physical processes must be involved. By giving the best result possible in the face of our uncertain knowledge of the parameters and observations, the optimal-fit procedure unambiguously indicates which oceanic features require model changes in order to be adequately characterized. Only in these cases can potential improvements be evaluated without improving the database.

1. Introduction

The work reported here is part of an ongoing effort to develop better simulation models of the ocean. From one point of view, developing a more thorough account of ocean physics is intrinsically virtuous. In view of the cost in computer time and research effort, however, attempts to improve model physics must be restrained by an assessment of the chances for success. We measure whether a new model is better by a comparison with data, evaluating the discrepancies between the model simulation and observations. Discrepancies could be due to either model shortcomings or errors in the data, most pointedly errors in the forcing data such as wind stress and cloud cover. In general, model shortcomings can be such that the form of the model is inadequate, in which case the model should be rebuilt, or they can be such that the form of the model is adequate, but the value of a poorly-known model parameter is poorly chosen. The latter sort of model shortcoming is relatively easy to repair, and one would like to avoid rebuilding the model until that possibility has been ruled out. Once good parameter choices have been made, however, discrepancies between calculated and observed variables are due either to model flaws that require rebuilding or to errors in the data. If the discrepancies are the size and structure expected of data errors, additional data are required to verify the model. If the discrepancies are larger or more structured than expected of data errors, then the data, although flawed, are good enough to allow *discernable* improvements in the model.

A specific example of an uncertain parameter representing more complicated physics is in our latent heat formulation. We use a constant "evaporation potential," which we know is not truly constant: a more complete formulation would replace it with a planetary boundary layer model which transports water vapor. Constructing one is a nontrivial undertaking, so before beginning we want to be sure the data will allow us to conclude that the effort was worthwhile: that the data will tell us it is discernably better than the present formulation.

In this paper we study a model for tropical sea surface temperature (SST) which includes representations of ocean dynamics, ocean thermodynamics, and surface heat exchange. We simultaneously optimize the values of those model parameters which are not well known a priori, using a procedure which takes explicit account of the uncertainties in the available data. The model–data discrepancies remaining after the parameters have been optimally chosen are analyzed to determine whether the present form of the model is adequate for its purpose: simulating tropical SST evolution.

Determining model parameters is a universal modeling problem. No ocean model, not even the most

* Lamont-Doherty Geological Observatory Contribution Number 4461.

Corresponding author address: Dr. Benno Blumenthal, Lamont-Doherty Geological Observatory of Columbia University, Palisades, NY 10964.

© 1989 American Meteorological Society

elaborate general circulation model (GCM), can include a complete representation of all ocean physics. Even if all the fundamental physics and computational dynamics are understood (which is close to the truth), it is still necessary to include the influence of subgrid scale processes on the larger scales which are retained. Attempts to do so rest on the assumption that these processes can be parameterized, which is not expected to be more than approximately true. Whether it is true enough depends on the particular goal.

A successful parameterization correctly represents the influence of its processes on the scales retained in the model. It usually depends on variables that are determined by the model, as well as variables determined from an external source such as measurements. Both sorts of variables have errors—the model variables because of the nature of the model, the data variables because of the nature of measurements—and the nature of the errors can greatly affect the success of a parameterization. For example, a precise parameterization which is critically dependent on a noisy measurement may perform worse than a crude parameterization which does not require this critical measurement. In creating a successful parameterization, then, one must not only consider the underlying processes, but also the nature of the model and the available data.

The work reported in this paper is directed toward the goal of improved simulation of tropical SST for the purpose of modeling interannual variability in the coupled ocean–atmosphere system. The ocean model used is not a GCM but a simpler model built for a specific purpose, the calculation of SST. This purpose requires attention to ocean dynamics and thermodynamics, and demands even closer attention to a submodel (i.e., a parameterization) for surface heat flux. The model is very much like that developed by Seager et al. (1988; henceforth SZC), which in turn evolved from the ocean model of Zebiak and Cane (1987). The Pacific Ocean version differs from these earlier versions in detail only; the Atlantic version is new.

Originally (Zebiak and Cane 1987) this ocean model was used as a component of an interactive ocean–atmosphere model. But here, as in SZC, the ocean–heat flux model pair is forced by observed surface wind and cloud cover (as well as by solar input, which is determined by time and latitude; SST is determined by the model). Our approach, however, is still conditioned by the goal of coupling to an atmospheric model. The standard bulk formulae are based on fits of direct flux measurements to local values of relatively measurable quantities like windspeed, SST, surface air temperature, relative humidity, cloudiness, position, and time. As in SZC, we avoid using observed surface air temperature and humidity because in the coupled system these boundary layer variables are largely determined by SST. Their roles in the conventional bulk formulae are taken by functions of SST in our parameterization. It would be better to incorporate fully the influence of the atmosphere on the marine surface layer, but this is beyond the scope of our present efforts.

In addition to the incompatibility with our modeling goals, specifying air–sea temperature differences and air humidity would introduce difficulties due to the nature of the available data as well. Apart from the results of a handful of microstructure and radiation measurements, there is no heat flux data. The fields of heat flux numbers which appear in atlases and as ocean model forcing are calculated from models; e.g., the bulk formulae. These models are based on isolated calibrations and are highly uncertain. Even if they were reliable, the data used to make atlases (and force our models), which comes from merchant ship observations, are of a distinctly lower quality than that used in the calibrations. Possibly it is too poor to provide usable estimates of the air–sea temperature and humidity *differences* which lie at the heart of these heat exchange parameterizations. At the very least the formulae should be recalibrated. The vast discrepancies in the heat flux numbers in different atlases indicate such data are not adequate for determining SST through heat flux based on conventional bulk formulae alone (cf. SZC).

Though both the ocean dynamics and heat flux formulation are greatly simplified, the model has been shown to do a creditable job of simulating tropical Pacific SST for both climatology (SZC) and low frequency variations (Seager 1989). These results suggest that the model does represent the physical processes most influential in determining SST. If we had specified surface heat flux values, the negative feedback control exerted on net surface heating by SST would have been lost, and the results testify to the dominant role of this feedback in determining SST. If we had taken the air temperature T_a from data, we would have constrained SST to be close to T_a, whereas in nature it is T_a which is forced to be close to SST: the ocean mixed layer has far greater thermal inertia than the planetary boundary layer. Specifying T_a would be little better than specifying SST directly; it would be no test of the model physics.

In addition to the data variables, a number of empirical constants appear in heat flux formulae—both ours and the standard bulk formulae. The values for these constants, which derive from a mixture of theory (e.g., for turbulent boundary layers) and a limited number of direct flux measurements, are quite uncertain (cf. SZC and references therein, especially Blanc 1987). In many cases they are only taken to be constant because information is too sparse to allow a more complicated representation.

Since there is virtually no heat flux data, one cannot find the empirical constants from a direct comparison with data. If one had perfect data and a perfect model for ocean thermodynamics, then the values of these constants could be determined by finding the heat flux

required to account for the observed SST changes. What we are able to do is make optimal *estimates* of the empirical constants by considering the heat fluxes in our model, estimates that take account of model and data errors.

It should be emphasized at the outset that these numbers emerge as a byproduct of our work. Our principle objective is to obtain guidance on where to invest our efforts to improve our model. There are many features of the model which obviously lack verisimilitude and invite elaboration. What is not obvious is whether or not the considerable effort needed to implement such "improvements" would pay off in a discernable improvement in the model's *raison d'etre,* the simulation of tropical SST.

The plan of the remainder of the paper is as follows. The next section discusses the physical processes included in modeling ocean dynamics, ocean thermodynamics, and surface heat flux. In most respects this follows SZC, but the representation of ocean dynamics is somewhat new, combining a conventional multimode model with a surface layer in a consistent way (the representation is worked out in detail in appendix A). Section 3 explains the statistical method, and section 4 presents the results of applying it to the tropical Atlantic and Pacific climatologies. The final section gives our conclusions.

2. Ocean model

The ocean model has three major parts: a linear, wind-driven model for the velocity and pressure fields, an advective/diffusive SST equation, and a parameterization for surface heat flux. The three parts are not completely interdependent: while SST and heat flux depend on each other and on the velocity and pressure fields, the velocity and pressure fields are independent of both the SST and heat flux fields.

a. Velocity and pressure

This part of the model consists of a surface mixed layer atop a linear equatorial beta-plane deep ocean. The motions of the deep ocean are projected onto a small number, N, of wind-forced vertical modes. The surface mixed layer adds to the modal circulation a direct Ekman flow and is of particular interest since it governs the SST evolution. The $N = 1$ version of the deep-ocean part of the model resembles the models of Cane (1979) and Schopf and Cane (1983), and is essentially that of Zebiak and Cane (1987) and SZC.

Our fundamental dynamical model is set on an equatorial beta-plane and linearized about a resting basic state, with stratification purely a function of depth. These assumptions are those underlying the usual linear theory which has proven successful in many applications to equatorial dynamics. Calculations employing the linear theory most often find the solution as a sum over N vertically standing modes. For some purposes it suffices to take $N = 1$ (e.g., Busalacchi and O'Brien 1981); for others N is quite large (e.g., $N = 60$ in McCreary 1981). In the present paper we have a model with a surface layer of fixed depth h_{mix} plus a small number, N, of vertical modes. The $N = 1$ version has been derived in the literature, but to our knowledge there is no prior discussion of the consistency of this formulation for $N > 1$. We pursue this point in appendix A, where it is shown that the surface layer dynamics are equivalent to summing over all the higher modes.

The model basin extends from 30°N to 30°S and otherwise covers the region indicated by the shading in Figs. 6–10. For the Atlantic, grid spacing is 1° in longitude and 0.5° in latitude and the timestep is one week. The model cannot handle all the irregularity of the Atlantic basin, and its lack of geometric fidelity makes it inappropriate for simulation of currents near the coasts. In the Pacific, grid spacing is 2° in longitude and 0.5° in latitude and the timestep is 10 days. In the Atlantic $h_{\text{mix}} = 35$ m; the mixed layer is deeper in the Pacific, $h_{\text{mix}} = 50$ m. In order to match SZC, the Pacific model has one mode with an equivalent depth of 86 cm, a phase speed of 2.9 m s^{-1}, and an effective depth $D_1 = 150$ m. The relatively small value of D_1 (see Cane 1984) compensates for the missing higher baroclinic modes. The Atlantic model has 5 modes; modal characteristics, based on a mean Atlantic profile, are summarized in Table 1. The values of r_n used for the model friction (cf. Gent et al. 1983, for a discussion) are too small to affect the solutions appreciably. The only remaining adjustable model parameter, the surface layer friction r_s, is assigned the value 0.5 days^{-1}; its influence is felt only near the equator for $|y| < r_s/\beta \approx 2.5°$.

b. Sea surface temperature

While the ocean model which governs velocity and pressure is linear and thus excludes the advection terms in the equations, the SST is determined from a fully nonlinear advective equation. The temperature is assumed to be uniform (well mixed) in the layer. The sea surface temperature T_s is then determined from the

TABLE 1. Dynamical Atlantic mode parameters.

Mode	Equivalent depth (m)	Horizontal phase speed (m s^{-1})	Length scale (km)	Time scale (days)	D_n (m)	Sea level amplitude (m)
1	0.568	2.36	322	1.58	348	1.91
2	0.194	1.38	246	2.06	145	1.02
3	0.083	0.89	199	2.56	429	0.26
4	0.049	0.69	175	2.91	603	0.13
5	0.029	0.53	153	3.32	440	0.09

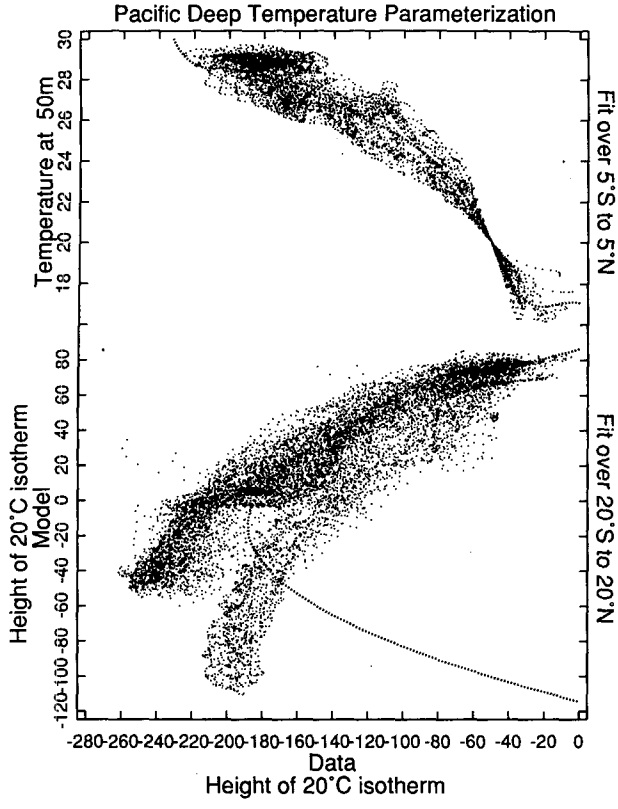

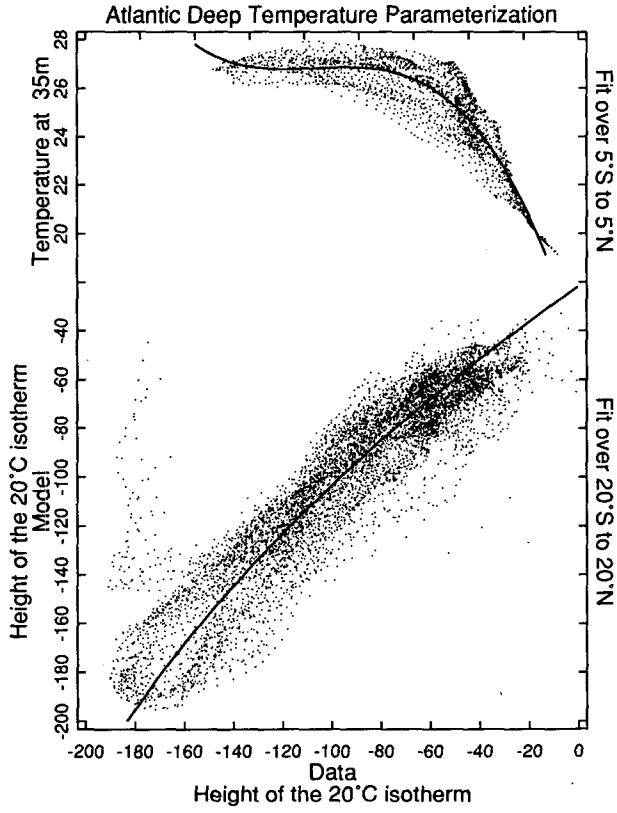

net balance of horizontal advection, upwelling, and the surface heat flux:

$$\partial_t(h_{\text{mix}}T_s) + u_T\partial_x(h_{\text{mix}}T_s) + v_T\partial_y(h_{\text{mix}}T_s) + \gamma w(T_s - T_d) = Q + \kappa(\partial_{xx} + \partial_{yy})(h_{\text{mix}}T_s) \quad (1)$$

where T_d is a subsurface temperature determined by the dynamics below the mixed layer. The upwelling term is usually written as $w(T_s - T_e)$, where T_e is the temperature of water entrained into the mixed layer. The two temperatures T_e and T_d are related by

$$T_e = (1 - \gamma)T_s + \gamma T_d. \quad (2)$$

Because the entrainment efficiency γ is less than one, the temperature of entrained water T_e is somewhere between the sea surface temperature T_s and the deep temperature T_d. The parameterization for the heat loss due to upwelling of cool water into the surface layer is thus dependent on an entrainment efficiency γ and a local deep temperature T_d, which should be at a depth beneath the base of the mixed layer [viz., (2)]. The model assumes the mixed layer is of fixed depth (50 m in the Pacific, 35 m in the Atlantic), and T_d is taken to be the local temperature at that depth. As in SZC, T_d is parameterized as a function of model thermocline depth [i.e., depth of the 20°C isotherm z(20°C)]. The parameterization is done in two parts: first the temperature at the mixed layer depth is fit to the depth of the 20°C isotherm using the Levitus (1982) dataset, then the depth of the 20°C isotherm is fit to the model's prediction of the thermocline depth h. This pair of empirical functions give T_d as a function of h.

In the Pacific, the empirical fit for T (50 m) as a function of z (20°C) is taken from SZC—it is given in the upper part of Fig. 1a. In the Atlantic, the fit for T (35 m) as a function of z (20°C) is computed as a best-fit cubic: it is given in the upper part of Fig. 1b. In both cases the fit is done with data from 5°N to 5°S. This narrow band was chosen because the depth of the 20°C isotherm ceases to be a good predictor of mixed layer depth temperature if data from a wider latitude band is included. While the fit is good in the equatorial band, it is rather poor for the basin as a whole. This is not necessarily a problem, however, because to the extent that upwelling occurs primarily on the equator the errors in deep temperature away from the equator are unimportant. If necessary, a spatial dependence could

FIG. 1. (a) Pacific deep temperature (T_d) parameterization. Top: Points show the observed temperature at 50 m vs the observed depth of the 20°C isotherm in the equatorial Pacific, 5°S–5°N, in all months. The line is the best fit of temperature as a function of depth. Bottom: The model calculated depth of the 20°C isotherm vs the observed depth for all points from 20°S to 20°N, together with the best fit quadratic curve. The fits are as in SCZ; all data is from Levitus (1982). (b) Atlantic deep temperature (T_d) parameterization. As in Panel (a), but for the Atlantic. The fit of temperature to depth is a cubic. Calculated 20°C depth is based on the 5 mode model.

be added to the parameterization of T_d without otherwise revising the model's structure.

Unlike the empirical fit for $T(50\text{ m})$ and $T(35\text{ m})$ as a function of 20°C isotherm depth $z(20°C)$, the fit of the model 20°C isotherm depth to the Levitus 20°C isotherm depth is quite good over a wide latitude range. The lower part of Fig. 1b shows the fit for a 5 mode Atlantic model for seasonal points between 20°N and 20°S. The fit is mostly within 20 m except for some poorly matched coastal points (the model thermocline shoals while the data thermocline does not). Note also that there is little curvature in the best fit line, especially when compared with the one mode Pacific model fit shown in the lower part of Fig. 1a. The difference in curvature is primarily due to extra modes in the Atlantic model, rather than any differences between the two oceans.

c. *Surface heat flux*

The surface heat flux parameterization is the same as in SZC. As SZC point out, since this surface heat flux parameterization is a forcing term for the SST evolution equation, it should only include effects that are truly externally imposed on the SST. Since the air temperature to a large extent is fixed by the SST, it has been eliminated as a parameter. This leaves wind speed and cloud cover as the only measurements in the heat flux calculation.

The surface heat flux is the sum of the solar flux, latent heat, sensible heat flux and back radiation. The clear sky solar flux Q_0 is determined from a formula that accounts for latitude and time of year. At the ocean's surface it is reduced by the effects of a constant surface albedo (0.06), measured cloud cover C, and the absorption and reflection of the atmosphere, which depends on solar angle α (cf. Weare et al. 1980). The latent heat flux is computed from the standard bulk formula using a fixed percentage a_{RH} of the saturation humidity $q_s(T_s)$ as the evaporation potential $\phi = q_s(T_s) - q_s(T_{air})$. The sensible heat flux and back radiation are modeled together as being proportional to the difference between the sea surface temperature T_s and a reference temperature T_0. This term is small relative to the solar and latent heat fluxes (Weare et al. 1980), having a variability of less than 20 W m^{-2} over the tropical Pacific, so an imprecise parameterization of this term does not significantly affect the results. The net surface heat flux is thus given by

$$Q = (0.94)Q_0(1 - a_C C + a_\alpha \alpha) - \rho_a C_E L |\mathbf{v}| a_{RH} q_s(T_s) - a_{sst}(T_s - T_0). \quad (3)$$

As discussed in SZC, $|\mathbf{v}|$ is not allowed to fall below 4 m s^{-1} in order to compensate for the loss of variability in using monthly winds.

This paper differs from SZC in that the parameters (a_C, a_α, a_{RH}, a_{sst}, T_0) are altered to optimize the model's reproduction of the climatological SST data. (We also tried varying the albedo and the minimum wind speed, but since these parameters were not altered by our procedures they will not be considered further.) The potential for optimization to improve parameter choices can be gauged by examining the relative importance of the different heat flux terms. Plotted in Fig. 2 are the mean values and doubled standard deviations for most of the model heat flux terms. The primary balance is between the solar input and the combined effects of cloudiness and latent heat flux. Consequently the coefficients of those terms are best determined by the optimization. The procedure for determining optimal parameter values and their significance in the presence of noise are discussed in the following sections.

3. Best fit of heat flux parameters

We wish to test whether the present model physics are adequate to model the SST data. The observed values of both forcing and verification data are imprecisely known and possibly in error. If the model agrees with the data to within expected error, it will be judged adequate. But a number of model parameters are not known precisely from experiment or theory, and the model should not be judged a failure because the parameter values are poorly chosen. At the same time, we do have some notion of the parameter values, so we do not wish to let them vary unconstrained. We thus perform a best-fit calculation, allowing the uncertain parameters to vary within their uncertainties, and then evaluate the remaining discrepancies between the model and data. This procedure only alters the

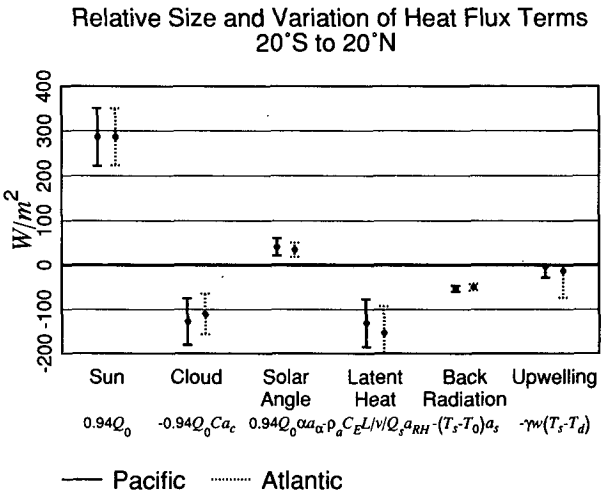

FIG. 2. Relative size and variation of heat flux terms in the surface heat balance, 20°S–20°N. On average, the solar input is balanced primarily by the effects of clouds and the latent heat loss to the atmosphere. The mean value of each term over the basin is given by the heavy dot and the rms deviations are given by the error bars. The solid lines are for the Pacific and the dotted lines are for the Atlantic.

values of the parameters if their a priori uncertainties are greater than the uncertainties due to the data. As it turns out, the results are mixed: some parameters are altered, reducing the discrepancy between model and data, and some parameters are not, leaving the discrepancy unchanged.

The surface heat flux parameterizations are quite uncertain, and uncertainties in the wind and cloud data would add noise to the estimates of surface heat flux even if the parameterizations were perfect. Relatively speaking, SST is well measured. From a data point of view, then, it makes sense to use the time evolution of SST to refine estimates of surface heat flux rather than use uncertain surface heat flux parameterizations to predict SST. Our a priori values for the model parameters to be varied (a_C, a_α, δ, a_{sst}, T_0, γ, C_D, κ) are taken from the literature; i.e., the values are from a mixture of theory and heat flux measurements. These a priori values are somewhat uncertain. The best-fit procedure varies the parameters within those uncertainties to reduce the corrective heat flux, the corrective heat flux being the heat flux necessary to make the model SST match the data SST exactly. As can be seen in Fig. 3, large corrective heat fluxes tend to precede large differences in SST.

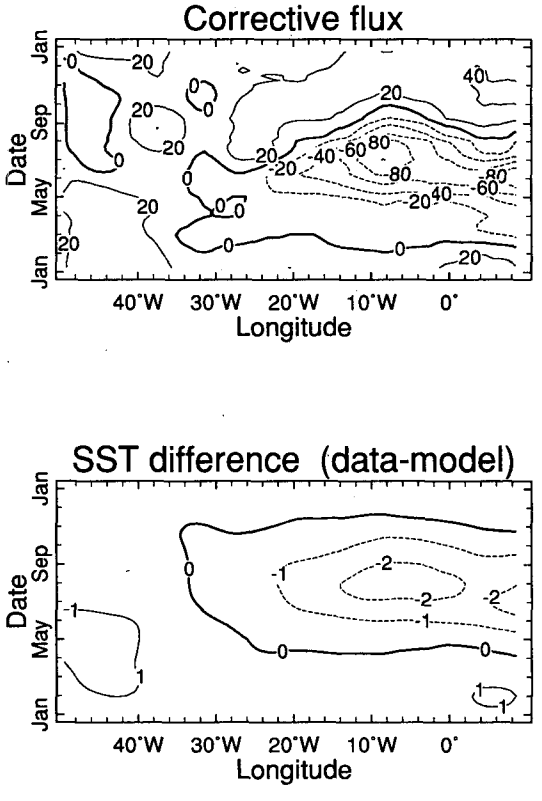

FIG. 3. Top, corrective heat flux (W m^{-2}). Bottom, data − model SST difference in the equatorial (5°S–5°N) Atlantic. Note the slight lag between the SST difference and the corrective heat flux necessary to force the model to track the data exactly.

a. Model equations

In the SST evolution equation's standard interpretation, horizontal advection, upwelling, and surface heat fluxes give the time evolution of the SST. Here we rewrite (1) as the following equation for the corrective heat flux:

$$\Delta Q = Q - \gamma w(T_s - T_d) - u\partial_x(hT_s) - v\partial_y(hT_s) - \partial_t(hT_s) + \kappa(\partial_{xx} + \partial_{yy})(hT_s), \quad (4)$$

where T_s is the SST given by the data, horizontal advection and upwelling are determined by the model circulation (which is determined by the wind forcing), and surface heat flux Q is determined via the parameterization (3) from wind data, cloud data, and SST data. An optimal set of model parameters is calculated by minimizing the rms ΔQ.

We are interested in how the corrective heat flux, ΔQ, depends on the parameters which are allowed to vary. An expression for this dependence at each point in space and time is obtained from (4) [with Q given by (3)], retaining only the terms that are affected by parameter changes. This determines a set of linear equations for $\delta\mathbf{q}$, the corrective heat flux at all space/time points:

$$\delta\mathbf{q} = \mathbf{M}\delta\mathbf{a}, \quad (5)$$

where the ith row of $\mathbf{M}$ (written $\mathbf{m}_i^{\mathrm{T}}$) represents the equation at the ith space/time point. Here $\mathbf{m}_i^{\mathrm{T}}$ and $\delta\mathbf{a}$ are given explicitly by

$$\mathbf{m}_i = \begin{bmatrix} -0.94Q_{0_i}C_i \\ 0.94Q_{0_i}\alpha_i \\ \rho_a C_E|\mathbf{v}_i|q_s(T_{si}) \\ -T_{si} \\ 1 \\ -w(T_{si} - T_d) \\ -u\partial_x(hT_s) - v\partial_y(hT_s) - \gamma w(T_{si} - T_d) \\ (\partial_{xx} + \partial_{yy})(hT_s) \end{bmatrix},$$

$$\delta\mathbf{a} = \begin{bmatrix} \delta a_C \\ \delta a_\alpha \\ \delta a_{\mathrm{RH}} \\ \delta a_{\mathrm{sst}} \\ \delta(a_{\mathrm{sst}}T_0) \\ \delta\gamma \\ \delta a_D \\ \delta\kappa \end{bmatrix}. \quad (6)$$

where δa_D represents the percentage change in the (wind) drag coefficient C_D, and a term proportional to $\delta a_D \delta\gamma$ has been dropped to linearize the model.

b. Best-fit procedure

Optimal estimates of the heat flux parameters are calculated from a best-fit procedure derived and discussed in Menke (1984), which combines the linear

model **M** with error information. The solution found is optimal given that the errors can be considered Gaussian and statistically independent. The cast of this statistical production is fairly large, so we would like to introduce each in turn:

- $\mathbf{M}^{(0)}$ is the true model matrix corresponding to **M**.
- $\mathbf{a}^{ap}$ are the a priori values of the model parameters—our initial notion of what the parameter values should be.
- $\mathbf{q}^{ap}$ are the corresponding a priori values of the heat flux, $\mathbf{q}^{ap} = \mathbf{M}\mathbf{a}^{ap}$.
- $\mathbf{a}$ are the true values of the parameters—this is what we would like to estimate.
- $\mathbf{q}$ are the correctly modeled values of the heat flux—they result from the true values of the model parameters using the true model $\mathbf{q} = \mathbf{M}^{(0)}\mathbf{a}$.
- $\mathbf{q}^{cur}$ are the current values of the heat flux; they are given by $\mathbf{q}^{ap} + \delta\mathbf{q}$, where $\delta\mathbf{q}$ are calculated according to (4) using $\mathbf{a}^{ap}$.
- $\mathbf{R}_\mathbf{a}$ is the error covariance of the a priori model parameters, i.e., the uncertainty of those values.
- $\mathbf{R}_\mathbf{q}$ is the error covariance of the difference between $\mathbf{q}$ and $\mathbf{q}^{cur}$—it characterizes the variability in $\mathbf{q}^{cur}$ that is external to the model **M**, e.g., subgrid scale phenomena, errors in the calculation of $\delta\mathbf{q}$. We will refer to this as the *irreducible uncertainty:* because it is external to the model, it cannot be reduced by model tuning and once the differences $\delta\mathbf{q}$ are that size we consider the model successful. Equivalently, we do not expect the parameterization to be more accurate than the level of error $\mathbf{R}_\mathbf{q}$.
- $\mathbf{R}_{\mathbf{Ma}}$ is the error covariance of the model matrix **M** projected onto the a priori values of the model parameters $\mathbf{a}^{ap}$, i.e., it is only the portion of the error covariance tensor of **M** that affects the calculation. The errors in **M** are primarily due to the data that is used to calculate its elements.

By considering the probability distributions that correspond to those quantities, we can construct an optimal estimator for the parameters **a**. Let $P(\mathbf{a})$, $P(\mathbf{q})$, $P(\mathbf{q}|\mathbf{a})$ be the probability distributions for the model parameters **a**, corrective flux **q**, and **q** given **a** respectively:

$$P(\mathbf{a}) \propto \exp[-(\mathbf{a} - \mathbf{a}^{ap})^T\mathbf{R}_\mathbf{a}^{-1}(\mathbf{a} - \mathbf{a}^{ap})/2]$$

$$P(\mathbf{q}) \propto \exp[-(\mathbf{q} - \mathbf{q}^{cur})^T\mathbf{R}_\mathbf{q}^{-1}(\mathbf{q} - \mathbf{q}^{cur})/2]$$

$$P(\mathbf{q}|\mathbf{a}) \propto \exp[-(\mathbf{q} - \mathbf{M}\mathbf{a})^T\mathbf{R}_{\mathbf{Ma}}^{-1}(\mathbf{q} - \mathbf{M}\mathbf{a})/2]. \quad (7)$$

We assume that the errors represented by $\mathbf{R}_\mathbf{q}$ are independent of the errors represented by $\mathbf{R}_{\mathbf{Ma}}$, something that is not necessarily true in practice.

The best-fit solution combines the model equations (5) according to the uncertainties given in the three probability distributions. In matrix form the solution can be written as (Menke 1984, p. 93)

$$\delta\mathbf{a} = \mathbf{B}\delta\mathbf{q}, \quad (8)$$

where

$$\mathbf{B} = [\mathbf{M}^T(\mathbf{R}_\mathbf{q} + \mathbf{R}_{\mathbf{Ma}})^{-1}\mathbf{M} + \mathbf{R}_\mathbf{a}^{-1}]^{-1}\mathbf{M}^T(\mathbf{R}_\mathbf{q} + \mathbf{R}_{\mathbf{Ma}})^{-1}. \quad (9)$$

The parameter changes presented in Fig. 4 are calculated using (8).

As noted above, three sources of uncertainty enter the best-fit procedure: uncertainties in the model parameters **a**, uncertainties in the model matrix **M**, and irreducible uncertainties in the corrective heat flux $\delta\mathbf{q}$. The best-fit procedure uses the three different sorts of uncertainties in different ways. The model parameter uncertainties $\mathbf{R}_\mathbf{a}$ are used to allocate between unresolved parameters: e.g., if there are two parameters that cannot be distinguished from each other by using the

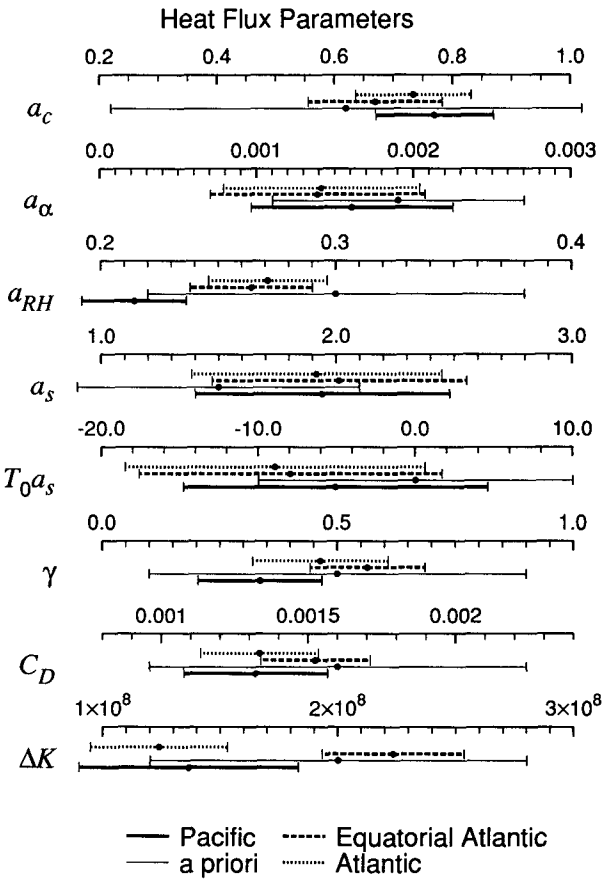

FIG. 4. The heat flux parameters for the optimal fits in the Atlantic and Pacific. The light solid error bars give the a priori value and doubled a priori error size for each parameter, the solid error bars give the estimate and doubled standard error for the Pacific, and the dotted error bars give the estimate and doubled standard error for the Atlantic. Error bars that are the same size as the a priori bars indicate poorly resolved parameters.

model **M**, then the best-fit makes a larger change in the more uncertain parameter. The sum of the model uncertainties $\mathbf{R}_{\mathbf{Ma}}$ and the irreducible uncertainties in the corrective fluxes $\mathbf{R}_{\mathbf{q}}$ determine the uncertainty of each equation $\mathbf{R} \equiv \mathbf{R}_{\mathbf{q}} + \mathbf{R}_{\mathbf{Ma}}$ and thus set the relative weight each space-time data point has in determining the new values of the parameters. Thus in computing the parameter correction estimates $\delta\mathbf{a}$ the uncertainties in the model and the uncertainties in the data are indistinguishable; viz., (9).

In computing the probable error of these estimates, however, those two uncertainties contribute in different ways. The covariance matrix corresponding to probable error in the parameter estimates is

$$\mathbf{B}\mathbf{R}_{\mathbf{q}}\mathbf{B}^{\mathrm{T}} + (\mathbf{I} - \mathbf{B}\mathbf{M})\mathbf{R}_{\mathbf{a}}(\mathbf{I} - \mathbf{B}\mathbf{M})^{\mathrm{T}} \qquad (10)$$

(see Menke 1984, p. 93). The first term is a direct component, the projection onto the parameters of the irreducible heat flux uncertainty. The second term is a lack of resolution component, which is the uncertainty remaining after the a priori parameter uncertainty has been reduced by using the available information as in (8). By reducing the resolution **BM**, uncertainties in the *model* increase the lack of resolution component of the probable error; the irreducible uncertainties both reduce the resolution and contribute directly through the direct component. Thus model uncertainties and irreducible uncertainties are somewhat distinguishable.

The a priori uncertainties in the model parameters $\mathbf{R}_{\mathbf{a}}$ were chosen to be uncorrelated and to have standard deviations of roughly 20%–30%; they are given in Fig. 4 (error bars labeled "a priori").

Because the data that goes into calculating $\delta\mathbf{q}$ and **M** is based on gridded versions of coarsely box-averaged datasets, the noise for neighboring grid points is quite correlated (the model grid being smaller than the scale of the noise). Consequently, both $\mathbf{R}_{\mathbf{q}}$ and $\mathbf{R}_{\mathbf{Ma}}$ have nondiagonal structure. We can model this correlation with a fairly simple form for the noise covariance, the noise covariance **R** between two points (x_1, y_1) and (x_2, y_2) being given by

$$R(x_1 - x_2, y_1 - y_2) \propto 2^{-|x_1-x_2|/L_x} 2^{-|y_1-y_2|/L_y}, \qquad (11)$$

where the half-power scales (L_x, L_y) are determined from the box-averaging scales in our case (though more generally they are determined from the scales of the noise). In appendix B it is demonstrated that given a noise covariance of the form (11) there is a diagonal matrix $\nu^{-1}\,\mathbf{R}_D$, which is equivalent to **R** in the sense that **B** and error estimates (10) are essentially unchanged by using it in place of **R**. The diagonal elements of $\mathbf{R}_D$ are taken to be the same as those of **R**. The error amplitude is then modified by a "degree of freedom factor" ν which is a function of the number of grid points in an error correlation scale: for grid sizes $(\Delta x, \Delta y)$, $\nu = \nu(L_x/\Delta x, L_y/\Delta y)$. The determination of length scale pairs and the corresponding ν values is discussed in appendix B, and the sensitivity of the calculation to ν is discussed below.

The uncertainties in the model $\mathbf{R}_{\mathbf{Ma}}$ have multiple sources. Blanc (1987) considers the error in estimates from a single set of ship observations using the bulk formulae. This differs somewhat from the estimates used here, since the estimates here are averages over fairly large areas. But much of Blanc's analysis is relevant for these large scale averages, since most of the uncertainty he finds is in the parameterization. As a rough approximation to the errors in the model matrix, (5) and the a priori mean values of the parameters were used to convert uncertainties in the data into uncertainties in heat flux. Uncertainty in the wind (0.75 m s^{-1}) leads to an uncertainty of 20 W m^{-2} in the latent heat flux and uncertainty in the clouds (0.1) leads to an uncertainty of 20 W m^{-2} in the effect of clouds on heat flux. The variance due to these two error sources dominate the other terms: The uncertainty in the sum of the other terms is close to 10 W m^{-2}.

The irreducible uncertainties $\mathbf{R}_{\mathbf{q}}$ are the error due to dynamics not included in the model, error that would exist even if the model coefficients **M** had no noise: in these calculations that error was estimated to be 10 W m^{-2}. Combining the uncertainties in the model coefficients and this remaining corrective flux error gives an rms equation error of roughly 35 W m^{-2}. This is somewhat higher than Weare's (1981) estimates (25 W m^{-2}), mainly because he considers the cloudiness data to be much more reliable than we do. It is only slightly smaller than Blanc's (1987) analysis would suggest, though our noise estimate does not explicitly include many of the effects that he discusses.

Here $\mathbf{R}_{\mathbf{a}}$ is taken to be diagonal: parameter uncertainties are uncorrelated. $\mathbf{R}_{\mathbf{q}}$ and $\mathbf{R}_{\mathbf{Ma}}$ have the form (9) with the correlation scales L_x and L_y determined from the averaging scales of the data. As shown in appendix B, choosing these scales is equivalent to choosing the degree of freedom factor ν. Application of the method provides a check on the choice of ν, because in practice ν must be sufficiently large to stabilize the calculation. Figure 5 illustrates the influence of ν on the estimates of two parameters for a Pacific run. Figure 5a shows the dependence of δa_{sst}, a poorly resolved parameter, while Fig. 5b shows the dependence of a_{RH}, a relatively well resolved parameter. In the case of the poorly resolved parameter, the estimates are highly dependent on the choice of ν. For small values of ν the estimates differ significantly from the range given a priori as reasonable. As ν is increased the estimate eventually falls within the a priori range, but not before the error bars also encompass zero. This contrasts with the well resolved parameter a_{RH}, where the estimates are distinguishable from zero for the entire range of ν, and the error bars are distinctly smaller than the a priori

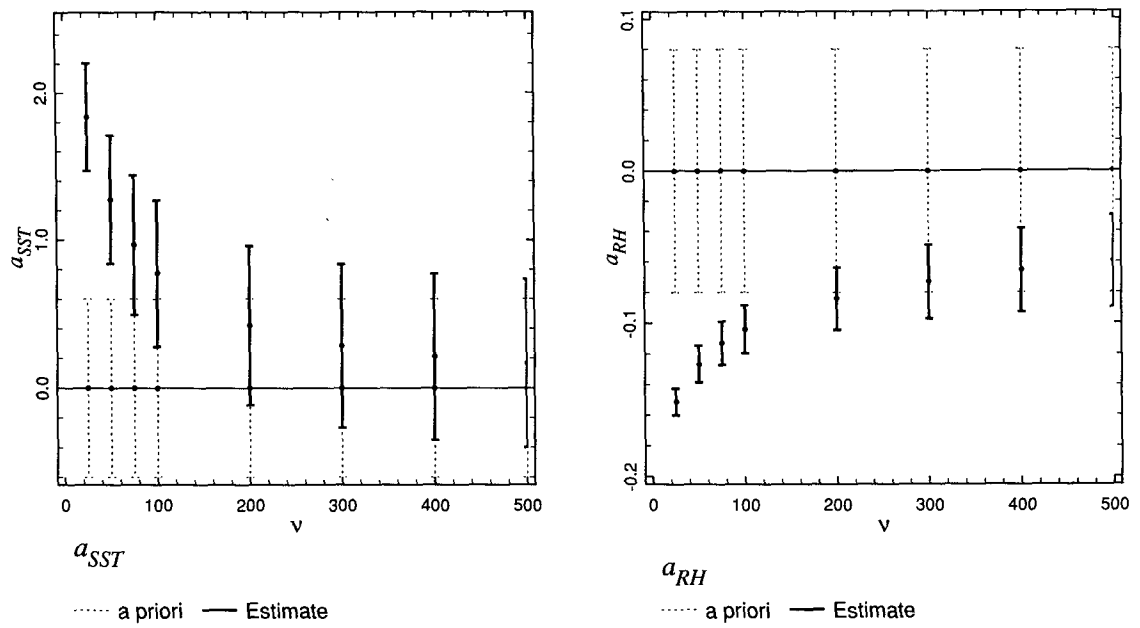

FIG. 5. Dependence of parameter estimates on ν, the reduction factor for the degrees of freedom. (a) The dependence for a_{SST}, a poorly resolved parameter. (b) The dependence for a_{RH}, a well-resolved parameter. The solid line indicated the estimate and its error bar (doubled standard deviation), while the dashed line gives the a priori estimate and the doubled a priori size. Shown here are deviations, i.e., the a priori mean has been removed.

range. On the basis of plots like these ν in the full-basin Pacific was chosen to be 200; in the full-basin Atlantic, 100. These choices are consistent with the values calculated from the noise scales in appendix B, O (170) and O (70) respectively.

4. Results

The tuning procedure is applied to sets of runs in both the Atlantic and Pacific. The runs require three sorts of data: wind stress, cloudiness, and SST. In both oceans the climatological cloudiness is taken from Esbensen and Kushnir (1981) (annual cycle), and the SST is taken from Climate Analysis Center (Reynolds 1982) averaged from 1970 to 1984. The wind stress in the Atlantic is based on the Hellerman wind product (Hellerman and Rosenstein 1983): a priori the stress is reduced by a factor of 0.75 to make the drag coefficient (C_D) closer to that suggested by Large and Pond 1981. (C_D is one of the parameters tuned in the fit: the results show that 0.75 is indeed a good choice). The wind (pseudo)stress in the Pacific is the annual cycle from the Florida State University wind product (Goldenberg and O'Brien 1981) averaged from 1961 to 1984. Runs were first made with the a priori values of the heat flux parameters. Maps from these runs are labeled "untuned" in Figs. 6–10. Those runs give corrective fluxes which are minimized to make optimal choices for the parameters. A second set of runs are then made using the optimal values of the parameters. Corresponding maps are labeled "tuned" in Figs. 6–10.

In both oceans the optimization procedure is applied to data from only the four months, January, April, July and October; using all 12 months would add little independent information. [Runs using 3-month averages gave essentially the same results as the four individual months.] Three runs are presented: a Pacific fit based on 20°S–20°N data ("Pacific"), an Atlantic fit based on the same range ("Atlantic"), and an Atlantic fit based on 10°S–10°N data ("Equatorial Atlantic"). In the Pacific, the tuning procedure reduced the corrective heat flux variance from 150% to 110% of the expected value [a variance which translates (square root) to an uncertainty of roughly 35 W m^{-2}]. In the Atlantic case, the tuning reduced the variance from 260% to 130% of the expected value, somewhat larger than the Pacific, and, as will be seen, more structured. The Equatorial Atlantic run was then made to see whether the high residues in the Atlantic indicated that parameter estimates were poor: the run reduced the corrective heat flux variance from 220% to 130% and for the most part gives similar parameter estimates, suggesting that the high residuals do not greatly influence most of the parameters.

Figure 4 summarizes the estimates for the parameters. Several of the coefficients were not determined by the optimization. This is seen in the plot when the range on the error bars is the same as the range on the a priori value (e.g., the solar angle parameter a_α and

the back-radiation parameters a_s and $T_0 a_s$). The other parameters are reasonably well resolved. The optimized choice for the cloudiness coefficient a_C is close in the two oceans, being somewhat larger than a priori value of 0.62, which is widely used (e.g., Weare et al. 1980). Relative evaporation potential a_{RH}, is (barely) significantly different between the two oceans, with the Atlantic estimates corresponding to drier air. In considering a_{RH} constant, the heat flux model has assumed that the moisture content of the air has equilibrated to the sea surface, a reasonable assumption sufficiently far from the coasts. Close to the coasts, however, when the wind is offshore, the air has not equilibrated, and it is somewhat drier than equilibrated air. The difference in estimates of a_{RH}, then, could result from coastal air being relatively important in the Atlantic, which is reasonable given that it is so much smaller than the Pacific. Note also that the coefficient a_{RH} subsumes changes in the exchange coefficient c_E as well as true changes in relative evaporation potential.

In the Pacific, the upwelling efficiency γ is somewhat smaller than the a priori value while the Atlantic values are essentially unchanged: the two oceans are, however, consistent with each other. This is not a particularly strong result: the mixed layer depths and the deep temperature parameterizations differ in the two oceans, differences that affect the interpretation of γ in the two oceans.

Drag coefficient changes (a_D) were fairly small (15% reduction) and identical in the two full basin fits. The a priori value of 1.6×10^{-3} includes a stability correction factor, thus it is somewhat larger than the low windspeed–neutral stability Large and Pond value of 1.2×10^{-3}. The "corrected" drag coefficient is

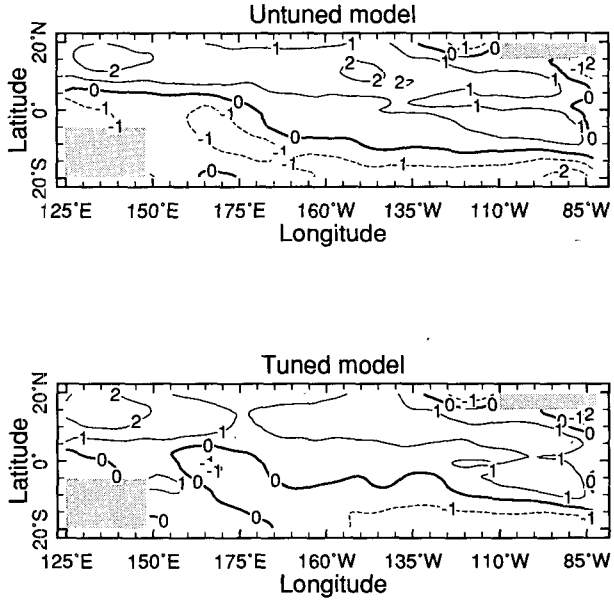

FIG. 6. April Pacific SST differences (data − model).

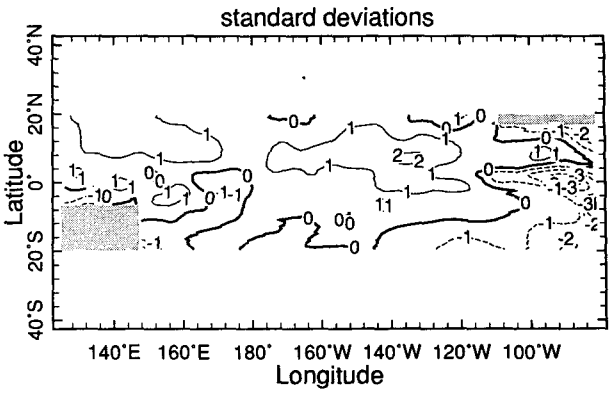

FIG. 7. April Pacific heat flux residuals in units of standard deviations.

$1.4(\pm 0.2) \times 10^{-3}$, interpretable as a 20% stability effect, a reasonable mean tropical value.

The diffusion coefficient estimates (κ) were the only ones to differ significantly between the Atlantic and Equatorial Atlantic runs. Since this term is particularly large near the coasts, and the Atlantic model is particularly bad near the coasts, it is likely that much of this estimate is a reflection of the poor job the model does near the coast, rather than an improved value of diffusion. The fact that the full basin models agree with each other and disagree with the Equatorial run suggests that, to the extent that diffusion can model coastal dynamics, a lower diffusion is required in coastal regions compared to equatorial regions. The conclusion that we draw, however, is that the model's ability to model coastal areas needs to be improved.

As mentioned earlier, in the Pacific the tuning reduced the overall corrective heat flux variance from 150% to 110% of expected. The improvement can also be seen in the difference in SST between data and model. Figure 6 shows that difference for a typical climatological month (April) in the Pacific. The untuned model has a tendency to be too cool in the north and the eastern equatorial region. The tuned model, on the other hand, matches quite well over the entire equatorial region, and only has differences as large as 2°C near coasts (which the model represents poorly) and near the northern extreme of the plot (which is reasonable given that the model is most correct for equatorial regions). The tuned model, then, gives distinctly better results than before.

Figure 7 shows the heat flux residuals for the Pacific estimation: this is the heat flux analog of the temperature difference maps in Fig. 6. These residuals can be interpreted as the changes necessary in the data needed to make the model and measured heat flux match. Since the inversion makes no distinctions between the sources of error in each equation (the total variance in the equation is the sum of the variances of the terms), one possible interpretation of the error results

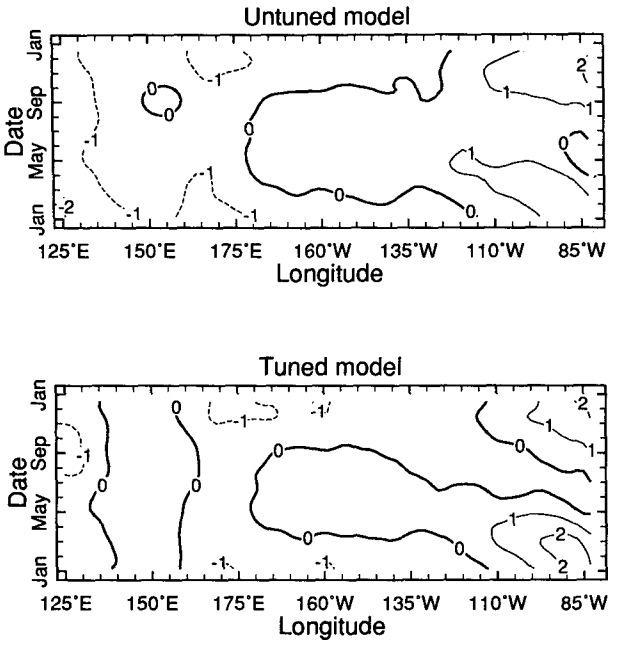

FIG. 8. Equatorial Pacific (5°S–5°N) SST differences (data − model).

is to spread the error equally among all the sources. In particular, a residual of one standard deviation means that a change of one standard deviation in each uncertain variable is sufficient to account for the difference, e.g., 0.75 m s^{-1} change in wind, 0.1 change in cloud fraction, 10 W m^{-2} in both upwelling and general heat flux error. This is equivalent to the total equation error of 35 W m^{-2}.

Figure 8 shows the difference in SST between data and model as a function of time for an equatorial band in the Pacific. The difference between tuned and untuned models is less striking from this perspective: the tuned model is better in the west and over much of the basin, while the untuned model is slightly better in the east in winter.

The tuning procedure also reduced the corrective heat flux in the Atlantic, from 260% of the expected noise variance to 130% of the expected noise variance. This is also seen in the SST differences. Figure 9 shows the SST difference for a climatological April in the Atlantic, while Fig. 10 shows the SST difference as a function of time for an equatorial band. The tuned model is much better in the equatorial region than the untuned version, but the results away from the equator are still poor. In particular, the model is too warm at the North African coast and near the Brazilian coast ("Cabo Frio"). The fact that large differences remain even after tuning shows that no reasonable change in the heat flux parameters could account for the differences. The fact that the remaining corrective heat flux is significantly larger than the expected value shows that errors in the data cannot explain the difference either. We conclude that there must be errors in the model. This is an important result, for it shows that the data, problem-ridden that it is, is sufficient to tell us something useful about the model. There are several model shortcomings that could account for errors with the structure shown in the figure. The poor representation of coastal geometry limits the accuracy of model surface currents and upwelling. The parameterization of latent heat flux assumes that the air temperature has equilibrated with the ocean temperature, which is less likely to be true at the coasts. Finally, and most easily corrected, the parameterization for the deep temperature is accurate only near the equator. This is not significant in the Pacific, where there is relatively little off-equatorial upwelling, but degrades the simulation in the Atlantic, where the off-equatorial upwelling is much more important. This would be correctable by using a deep temperature parameterization that has some horizontal dependence.

5. Conclusions

This paper compares an imperfect model with an imperfect dataset in both the Atlantic and the Pacific. In the Pacific, the differences between the model SST and data SST can be explained with changes in the heat flux that are the same size as the overall uncer-

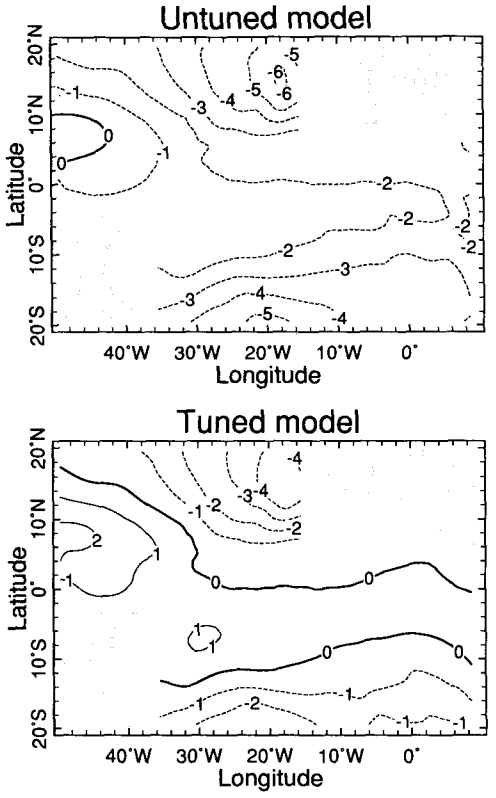

FIG. 9. April Atlantic SST differences (data − model).

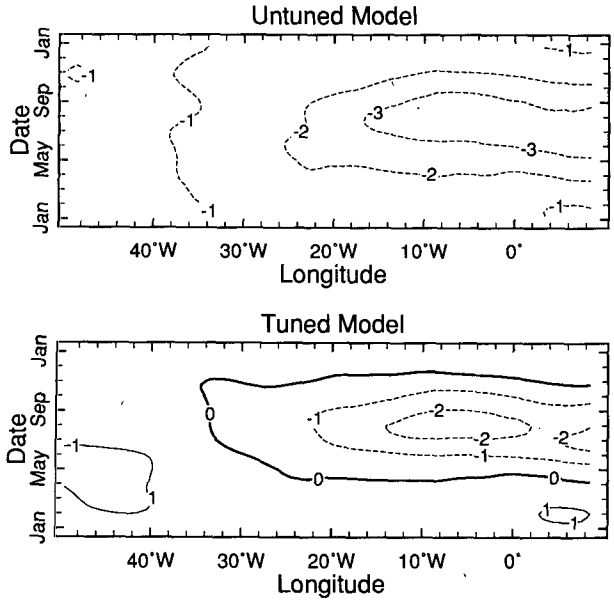

FIG. 10. Equatorial (5°S–5°N) Atlantic SST differences (data − model).

tainty in the heat flux, O(35 W m^{-2}). The results suggest some small changes in the heat flux parameters, namely that the coefficient for cloudiness a_C be changed from 0.62 to 0.76 ± 0.1 (95% confidence level) and that if the relative evaporation potential a_{RH} is going to be constant it should be given a value of 0.22 ± 0.02. In the Atlantic, the differences between the model and data are so great that they cannot be explained by modifying the heat flux formulation, and other physical processes and model problems must be considered.

These results show that while the physics included in the model are adequate to model SST in the Pacific, they are not adequate for the Atlantic. Why are the two oceans different? The Atlantic SST difference patterns (Fig. 9) suggest at least one reason. The patterns show that the boundary regions are particularly poorly modeled, especially the west African and southeastern Brazil coasts. To the extent that the model physics best represent the open ocean, trouble with boundary regions is not unexpected. Because the Pacific is so much larger than the Atlantic, the coastal regions are less influential, and an open ocean model does relatively well. In subsequent work, then, the effects of changes in the Atlantic *ocean* model will be investigated, with particular attention to coastal regions.

Should the heat flux parameters which emerge as a byproduct of our model validation procedure be regarded as anything more than an artifact of our model's idiosyncrasies? Of course, the bulk formulae are also models which vary from modeler to modeler [cf. SZC; one telling example is to compare the widely accepted drag coefficient of Hellerman and Rosenstein (1983) with the widely accepted version of Large and Pond (1981)], but the model here is decidedly indirect and is not even the most complete model available—it makes many gross simplifications of ocean structure.

While one could argue that our model performs as well as any other on its chosen problem, and thus is state-of-the-art, that is not really the point. We accept the fact that our numbers depend on our particular formulations of ocean dynamics, ocean thermodynamics, and surface heat flux, even on the particular datasets we have used. In fact, we embrace it: we believe that parameterizations are inherently dependent on the models and datasets with which they are used. Thus we recommend that the conventional heat flux formulae be used only as a starting point, from which modelers should calculate their own parameter values specific to their models and datasets.

At the same time, we cannot rule out the possibility that the values found here are more universal than might first appear. The procedure involves tuning only a few parameters from a large dataset, and their possible values are restricted a priori to a physically plausible range; that is, they are consistent with prior estimates in the literature to within the uncertainties in the latter. We do not claim that our formulae are universal; this possibility can only be evaluated empirically by trying our technique in the context of other models and other datasets. Our guess would be that any decent model would give about the same values if used with the same forcing and verification data, but that different data could very well lead to different numbers. In our experience, differences in surface wind fields are especially troublesome.

The tuning procedure allowed us to distinguish problems in the model from uncertainties in the data and parameterizations. Since all models have tunable parameters this technique may be applied to any in a hierarchy of models. We anticipate applying it to a primitive equation model (Gent and Cane 1988) in the near future and hope that the experience gained here will serve us well in a more complicated context. If the model was good enough, then this technique would allow us to give a useful estimate of surface heat fluxes (something we have thus far assiduously avoided), together with error bars.

It is naive, however, to presume that carrying on with a more complete ocean model will necessarily yield better estimates. Our present model sidesteps a number of potential pitfalls by *specifying* aspects of the ocean to be in good agreement with data: it is, in part, a diagnostic model. For example, we assume a constant mixed layer depth of 50 m in the Pacific. While not correct, this is not far from correct anywhere. One might do worse with a more complete parameterization which tries to account for depth variations. Perhaps the mixed layer model would be unable to handle some situation, or perhaps the demands it makes would be more than available data can bear. Ultimately, we will

want to use the most complete GCM, but that day has not yet arrived.

Acknowledgments. We would like to thank Richard Seager and Larry Carroll for furnishing earlier versions of the model, and providing computing assistance. We would also like to thank Virginia DiBlasi for typing the final version of the manuscript. This work was supported by NSF Grant OCE 86-08386, NASA Grant NAGW-916, and JPL Grant JPL957647.

APPENDIX A

Summing High Modes to Form a Surface Layer

The variables describing the ocean circulation may be written as sums of vertically standing eigenmodes; these expansions for the horizontal velocity components and the pressure are written as

$$\begin{bmatrix} u \\ v \\ \frac{1}{\rho} P \end{bmatrix} (x, y, z, t) = \sum_{m=0}^{\infty} \begin{bmatrix} u_m \\ v_m \\ gh_m \end{bmatrix} (x, y, t) A_m(z), \tag{A1}$$

where $A_m(z)$ is related to the mth eigensolution of the vertical structure equation, namely $A_m(z) = \partial_z G_m(z)$ and

$$\partial_{zz} G_m(z) + \frac{N^2(z)}{c_m^2} G_m(z) = 0. \tag{A2}$$

(Our notation follows Cane 1984).

We would like to use the special properties of a surface mixed layer to convert the infinite sum of modes into the sum of a few modes and some mixed layer dynamics. We will assume that there is a surface mixed layer of depth h_{mix}; in terms of horizontal velocity structure functions $A_m(z) = A_m(0)$ for $z > -h_{\text{mix}}$. We further assume that the stress τ vanishes below the mixed layer.

Introducing the form (A1) into the zonal momentum equation after ignoring the barotropic mode $m = 0$ (see Cane 1984) yields

$$\sum_{m=1}^{\infty} \partial_t u_m A_m - \beta y \sum_{m=1}^{\infty} v_m A_m + g \sum_{m=1}^{\infty} \partial_x h_m A_m = \partial_z \tau^{(x)} + \sum_{m=1}^{\infty} u_m F(A_m), \tag{A3}$$

where F is an operator, presumed linear, accounting for vertical mixing. Horizontal mixing is neglected, though its inclusion would have no effect on our argument.

By projecting onto individual modes, the single equation (A3) relating sums can be changed to a series of equations without sums. To obtain the equation for mode n, multiply (A3) by $A_n(z)$, integrate over the entire water column (depth D), and use the orthogonality of the $\{A_n(z)\}$; the result is,

$$\partial_t u_n - \beta y v_n + g \partial_x h_n = \tau_n^{(x)} - \sum_m r_{n,m} u_m, \qquad n = 1, 2, \cdots, \tag{A4}$$

where we have made use of the orthogonality condition

$$\frac{1}{D} \int_{-D}^{0} A_n(z) A_m(z) = \delta_{nm}$$

and have defined

$$\tau_n^{(x)} = \tau^{(x)} \cdot A_n(0)/D$$

$$r_{n,m} = \frac{1}{D} \int_{-D}^{0} A_n(z) F[A_m(z)] dz.$$

We are only interested in applying this projection for low modes, i.e., $n < N$. We will assume that for $n < N$, $r_{n,m} = 0$ for $m \neq n$ and write r_n for $r_{n,n}$ hereafter. This assumption is a more general but still artificial variant of the special treatment of friction in previous linear modal models (e.g., McCreary 1981 or Gent, O'Neill and Cane 1983); it allows us to recover the familiar form of (A4), in which friction appears only as Rayleigh friction and there is no coupling among different modes:

$$\partial_t u_n - \beta y v_n + g \partial_x h_n = \tau_n^{(x)} - r_n u_n \qquad n = 1, 2, \cdots, N. \tag{A5}$$

Define the total velocity contribution from high modes ($n > N$) as

$$(u_s, v_s) = \sum_{n=N+1}^{\infty} (u_n, v_n) A_n(z).$$

The result of subtracting $\sum_{n=1}^{N}$ [Eq. (A5)] $A_n(0)$ from (A3) can then be written ($z > -h_{\text{mix}}$)

$$\partial_t u_s - \beta y v_s + \left[\frac{1}{\rho} \partial_x P - g \sum_{n=1}^{N} \partial_x h_n A_n(0) \right] = \tau^{(x)} \left[\frac{1}{h_{\text{mix}}} - \sum_{n=1}^{N} \frac{1}{D_n} \right] + \{ F(u_s) + \sum_{n=1}^{N} u_n [F(A_n(0)) - r_n A_n(0)] \}, \tag{A6}$$

where we have written $\tau_n A_n(0) = \tau / D_n$, i.e., $D_n = D / A_n^2(0)$. Note that we have used the relation

$$1/h_{\text{mix}} = \sum_{n=1}^{\infty} D_n^{-1},$$

which follows from projecting a step function onto all modes and summing. The term in curly brackets on the rhs accounts for vertical friction and we have few qualms about treating it cavalierly. In line with previous

assumptions we take the term involving the sum to be negligible. The other term will be written in the simplest manner possible, as a Rayleigh friction:

$$F(u_s) = -r_s u_s.$$

The bracketed term on the left-hand side is concerned with the pressure gradient at the surface, or, equivalently, with the slope of sea level. It has been shown in a number of contexts (e.g., Cane 1984; Busalacchi and Cane 1985; duPenhoat and Treguier 1985) that sea level variations are well represented by a very few modes; perhaps as few as two. We will take N sufficiently large so that the bracketed term is negligibly small. After defining

$$\frac{1}{H_*} = \frac{1}{h_{\text{mix}}} - \sum_{n=1}^{N} \frac{1}{D_n}, \tag{A7}$$

(A6) can be rewritten

$$\partial_t u_s - \beta y v_s = \frac{\tau^{(x)}}{H_*} - r_s u_s. \tag{A8a}$$

A similar analysis of the meridional momentum equation leads to

$$\partial_t v_s + \beta y u_s = \frac{\tau^{(y)}}{H_*} - r_s v_s. \tag{A8b}$$

As they stand, Eqs. (A8a, b) are readily solved for (u_s, v_s) given the wind stress. Since we are only interested in low frequency motion (the wind data is monthly) the time dependent term is unimportant and may be neglected. Then (A8a, b) are just the equations for Ekman transport over an effective layer depth H_*. The Rayleigh friction term is important only near the equator where $\beta y < r_s$; it is there that the Ekman relations breakdown.

Thus, though the model takes the form of N vertical modes plus a surface layer, it is equivalent to an approximate solution of the infinite number of modes formulation of the standard linear equations (albeit with a particular form for the friction—but there is no standard choice here). We have exploited the fact that the modal series for the surface pressure converges very rapidly to derive the simple form (A8) for the sum of the higher modes ($n > N$) in the surface layer. Note that the series for u converges less rapidly: the scaling relation between h and u_n is $h_n = (H_n/g)^{1/2} u_n$ (cf. Cane 1984), where H_n, the equivalent depth, is a decreasing function of n. The last column of Table 1 indicates the influence of each mode on sea level and hence on the surface pressure gradient (cf. Cane 1984). The rapid decrease with mode number shows that these few modes account for P. For the low modes the wind stress is largely balanced by the pressure gradient force, while for the high modes it is balanced by Coriolis or friction terms. This qualitative difference was pointed out by McCreary (1981), who identified the low mode number balance with Sverdrup dynamics and the high n balance with the Yoshida solution.

The numerical procedure for finding

$$u_T = u(z = 0) = u_s + \sum_{n=1}^{N} u_n A_n(0) \tag{A9}$$

consists of solving for u_s from the steady state form of (A8) and solving for each of the u_n, $n = 1, N$ with the scheme devised by Cane and Patton (1984) as augmented by duPenhoat et al. (1983) to allow a less restricted basin geometry.

APPENDIX B

Interpreting the Degrees of Freedom Factor ν

In the body of this paper we have approximated the data space (equation) covariance $\mathbf{R} = \mathbf{R_q} + \mathbf{R_{Ma}}$ as a diagonal matrix $\mathbf{R}_D$ where the diagonal of $\mathbf{R}_D$ is copied from the diagonal of $\mathbf{R}$ normalized by the factor ν which reduces the resulting excess number of degrees of freedom $[R_D]_{ii} = \nu[R]_{ii}$. Here we demonstrate that a reasonable choice of ν induces minimal error in the inversion as represented by the matrix $\mathbf{B}$. We also develop the connection between ν and the correlation scales implicit in the noise covariance $\mathbf{R}$.

We first note that the resolution matrix $\mathbf{BM}$ relates the true value of the parameters $\mathbf{a}_0$ to their estimate $\mathbf{a}_{\text{est}}$, namely

$$\mathbf{a}_{\text{est}} = \mathbf{BM}\mathbf{a}_0. \tag{B1}$$

This is based on the idea that, as long as the model is valid, the true data $\mathbf{q}_0$ can be written in terms of the true model parameters, $\mathbf{q}_0 = \mathbf{M}\mathbf{a}_0$. Thus, we can understand the effects of using the diagonal covariance matrix $\mathbf{R}_D$ on the inversion by understanding the effect on the resolution matrix $\mathbf{BM}$. Writing out the resolution matrix explicitly,

$$\mathbf{BM} = [\mathbf{M}^T\mathbf{R}^{-1}\mathbf{M} + \mathbf{R_a}^{-1}]^{-1}\mathbf{M}^T\mathbf{R}^{-1}\mathbf{M}, \tag{B2}$$

we see that it only depends on the equation covariance $\mathbf{R}$ through the expression $\mathbf{M}^T\mathbf{R}^{-1}\mathbf{M}$. It is this expression, then, that we will use to evaluate choices of ν.

Since we in fact know very little about the structure of the noise covariance, it is fairly reasonable to choose a simple exponential form (11),

$$R(x_1 - x_2, y_1 - y_2) = 2^{-|x_1 - x_2|/L_x} 2^{-|y_1 - y_2|/L_y}. \tag{B3}$$

We use 2 rather than e so that the length scales (L_x, L_y) are the scales such that the normalized covariance (squared correlation) is 1/2. If we now grid the model with an x-coordinate spacing Δx and a y-coordinate spacing Δy, we can define single gridstep correlation factors

$$r = 2^{-\Delta x/L_x}, \quad s = 2^{-\Delta y/L_y}. \tag{B4}$$

a. One-dimensional grid

Consider for the moment the one-dimensional problem (coordinate x). Using n as the number of gridpoints, we can explicitly write the equation noise matrix $\mathbf{R}_x$ and a (one column) model matrix $\mathbf{M}$,

$$\mathbf{R}_x = \begin{bmatrix} 1 & & & & \\ r & 1 & & & \\ r^2 & r & 1 & & \\ \vdots & & & & \\ r^{n-1} & \cdots & r^2 & r & 1 \end{bmatrix}, \quad \mathbf{M} = \begin{bmatrix} m_1 \\ m_2 \\ \vdots \\ m_{n-1} \\ m_n \end{bmatrix}. \tag{B5}$$

[Covariance matrices (like $\mathbf{R}_x$) are symmetric: here only the lower triangle of a symmetric matrix is explicitly written.] $\mathbf{R}_x$ is easily invertible because of its special form,

$$\mathbf{R}_x^{-1} = \frac{1}{1-r^2} \begin{bmatrix} 1 & & & & \\ -r & 1+r^2 & & & \\ 0 & -r & & & \\ \vdots & & & 1+r^2 & \\ 0 & \cdots & 0 & -r & 1 \end{bmatrix}. \tag{B6}$$

The expression $\mathbf{R}_x^{-1}$ can also be written in a less clear but more explicit form,

$$[r]_{ij}^{-1} = \frac{1}{1-r^2}[(1+r^2)\delta_{ij} - r^2(\delta_{i1}\delta_{j1} + \delta_{in}\delta_{jn}) - r\delta_{ij+1}\delta_{i+1j}]. \tag{B7}$$

We can now compute the triple matrix product $\mathbf{M}^T\mathbf{R}_x^{-1}\mathbf{M}$,

$$\mathbf{M}^T\mathbf{R}_x^{-1}\mathbf{M} = \frac{1}{1-r^2}\left[\sum_{i=1}^{n}(1+r^2)m_i^2 - r^2(m_1^2+m_n^2) - 2r\sum_{i=1}^{n-1} m_i m_{i+1}\right]. \tag{B8}$$

We would like to compare this to the triple product computed with the diagonal matrix $\mathbf{R}_D$,

$$\mathbf{M}^T\mathbf{R}_D^{-1}\mathbf{M} = \frac{1}{\nu}\sum_{i=1}^{n} m_i^2. \tag{B9}$$

The expression (B8) can be simplified somewhat by making an approximation and a definition. The approximation is to approximate the boundary term as a fraction of the mean square, i.e.,

$$m_1^2 + m_n^2 \approx \frac{2}{n}\sum_{n=1}^{n} m_i^2. \tag{B10}$$

This term is a rather small contribution for large n, and would get dropped entirely if this approximation did not result in a simpler expression. We also define a scale ratio σ as

$$\sigma \equiv \frac{1 - \langle m_i m_{i+1}\rangle / \langle m_i m_i\rangle}{1-r}, \tag{B11}$$

where

$$\langle m_i m_{i+1}\rangle \equiv \frac{1}{n-1}\sum_{i=1}^{n-1} m_i m_{i+1}$$

$$\langle m_i m_i\rangle \equiv \frac{1}{n}\sum_{i=1}^{n} m_i m_i.$$

As can be seen in (B11), σ relates the single gridstep correlation of the model to the single gridstep correlation of the noise (r), such that $\sigma \ll 1$ is equivalent to the model scale being much longer than the noise scale.

We can now calculate what ν has to be to make (B8) and (B9) match; explicitly,

$$\nu \approx \left[\frac{1-(1-2/n)r}{1+r} + \frac{2r(1-1/n)}{1+r}\sigma\right]^{-1}. \tag{B12}$$

Note that for $r = 0$, $\nu = 1$, i.e., there is no degree of freedom reduction if all the data is independent. Another interesting limit is $r = 1$ and $\sigma = 0$, i.e., all the data is redundant and the model treats all data identically. In that limit $\nu = n$, i.e., the degree of freedom reduction is complete.

b. Two-dimensional grid

The two-dimensional generalization of the one-dimensional result is straightforward. The covariance matrix $\mathbf{R}_{xy}$ can be written as $(k \times k)$ matrix whose elements are the x coordinate matrices $\mathbf{R}_x$ defined by (B5);

$$\mathbf{R}_{xy} = \begin{bmatrix} \mathbf{R}_x & & & & \\ s\mathbf{R}_x & \mathbf{R}_x & & & \\ s^2\mathbf{R}_x & s\mathbf{R}_x & \mathbf{R}_x & & \\ \vdots & & & & \\ s^{k-1}\mathbf{R}_x & \cdots & s^2\mathbf{R}_x & s\mathbf{R}_x & \mathbf{R}_x \end{bmatrix}, \tag{B13}$$

i.e., this is an $(n \times k) \times (n \times k)$ matrix whose elements are scalars. Written as a matrix of matrices, however, makes it clear that the inverse is

$$\mathbf{R}_{xy}^{-1} = \frac{1}{1-s^2}\begin{bmatrix} \mathbf{R}_x^{-1} & & & & \\ -s\mathbf{R}_x^{-1} & (1+s^2)\mathbf{R}_x^{-1} & & & \\ 0 & -s\mathbf{R}_x^{-1} & & & \\ \vdots & & & (1+s^2)\mathbf{R}_x^{-1} & \\ 0 & \cdots & 0 & -s\mathbf{R}_x^{-1} & \mathbf{R}_x^{-1} \end{bmatrix}. \tag{B14}$$

Proceeding as in the one-dimensional case, it now follows that the two-dimensional version of ν is simply the product of the one-dimensional versions:

$$\nu \approx \left[\frac{1-(1-2/n)r}{1+r} + \frac{2r(1-1/n)}{1+r}\,\sigma\right]^{-1} \times \left[\frac{1-(1-2/k)s}{1+s} + \frac{2s(1-1/k)}{1+s}\,\sigma\right]^{-1}. \quad \text{(B15)}$$

One interpretation of these results is that there is an equivalent ν for every pair of noise correlation scales. Given what we know about the data, we can estimate these scales and compare the resulting ν to that used in the body of the paper. Since the dominate contributors to the noise are the wind (through the evaporative heat flux term) and the cloudiness (through its reduction of the solar input), one would expect the scales in those datasets to dominate ν. In the Pacific, the wind is calculated from the FSU product (Goldenberg and O'Brien 1981) which is based on an analysis of data that has been gridded to 10° × 2° boxes. That data has been contoured and then regridded, so we would expect the data to be even smoother than the original 10° × 2° might lead us to believe. Using a simplified version of (B15), which is appropriate for the large number of grid points and relatively uniform model,

$$\nu \approx \left[\frac{1+r}{1-r}\right]\left[\frac{1+s}{1-s}\right], \quad \text{(B16)}$$

and knowing that the Pacific model grid is 2° × 0.5°, we see that the corresponding ν would be 170, not much different than the 200 found by looking at the results of the inversion. The Atlantic wind data is taken from the Hellerman wind product (Hellerman and Rosenstein 1983): it is based on data box-averaged to a 2° × 2° grid, with some interpolation done for data poor regions. Most of the 20°S to 30°N band modeled in the Atlantic is not data poor, so except for the 30°S to 20°S range, 2° × 2° is a reasonable choice of scale for the data. The Atlantic model grid is 1° × 0.5°, so the corresponding ν value is 70, not far from the value used in the inversion (100), and the correction for the 30°S to 20°S range would reduce the difference. The cloudiness data for both oceans is taken from Esbensen and Kushnir (1981): it is based on 5° × 5° gridded data that has been smoothed using an objective analysis scheme which averages over all points within a 1100 km radius. Consequently the cloudiness data is much smoother than the wind data, and the corresponding ν factors are high: a 5° × 5° grid corresponds to ν = 200 in the Pacific and ν = 400 in the Atlantic. It is thus the smaller scales left in the wind that is the source of the variability which determines the effective number of degrees of freedom.

REFERENCES

Blanc, T. V., 1987: Accuracy of bulk method determined flux, stability, and sea surface roughness. *J. Geophys. Res.*, **80,** 3867–3876.

Busalacchi, A. J., and J. J. O'Brien, 1981: Interannual variability of the equatorial Pacific in the 1960s. *J. Geophys. Res.*, **86,** 10 901–10 907.

——, and M. A. Cane, 1985: Hindcasts of sea level variations during 1982/83 El Niño. *J. Phys. Oceanogr.*, **15,** 213–221.

Cane, M. A., 1979: The response of an equatorial ocean to simple wind stress patterns. II: Numerical results. *J. Mar. Res.*, **37,** 355–398.

——, 1984: Modeling sea level during El Niño. *J. Phys. Oceanogr.*, **14,** 586–606.

——, and R. J. Patton, 1984: A numerical model for low-frequency equatorial dynamics. *J. Phys. Oceanogr.*, **14,** 1853–1863.

duPenhoat, Y., and A. M. Trequier, 1985: The seasonal linear response of the tropical Atlantic ocean. *J. Phys. Oceanogr.*, **15,** 316–329.

——, M. A. Cane and R. J. Patton, 1983: Reflections of low frequency equatorial waves on partial boundaries. *Mem. Soc. R. Sci. Liege,* **6(XIV),** 237–329.

Esbensen, S. K., and V. Kushnir, 1981: The heat budget of the global ocean: An atlas based on estimates from surface marine observations. Climate Research Institute Rep. 29, Oregon State University, 27 pp.

Gent, P. R., and M. A. Cane, 1988: A reduced gravity, primitive equation model of the upper equatorial ocean. *J. Comput. Phys.*, in press.

——, K. O'Neill and M. A. Cane, 1983: A model of the semi-annual oscillation in the equatorial Indian Ocean. *J. Phys. Oceanogr.*, **13,** 2148–2160.

Goldenberg, S. B., and J. J. O'Brien, 1981: Time and space variability of tropical Pacific wind stress. *Mon. Wea. Rev.*, **109,** 1190–1207.

Hellerman, S., and M. Rosenstein, 1983: Normal monthly wind stress over the world ocean with error estimates. *J. Phys. Oceanogr.*, **13,** 1093–1104.

Large, W. G., and S. Pond, 1981: Open ocean momentum flux measurements in moderate to strong winds. *J. Phys. Oceanogr.*, **11,** 324–336.

Levitus, S. E., 1982: *Climatological Atlas of the World Ocean.* NOAA Professional Paper 13, U.S. Govt. Printing Office, 173 pp.

McCreary, J. P., 1981: A linear stratified ocean model of the equatorial undercurrent. *Phil. Trans. Roy. Soc., London,* **A298,** 603–635.

Menke, W., 1984: *Geophysical Data Analysis: Discrete Inverse Theory.* Academic Press.

Reynolds, R. W., 1982: A monthly averaged climatology of sea surface temperature. NOAA Technical Rep. NWS 31, National Weather Service, Silver Spring, MD, 35 pp.

Schopf, P. S., and M. A. Cane, 1983: On equatorial dynamics, mixed layer physics and sea surface temperature. *J. Phys. Oceanogr.*, **13,** 917–935.

Seager, R., 1989: Modeling the sea surface temperature of the tropical Pacific between 1970 and 1987. *J. Phys. Oceanogr.*, **19,** 419–434.

——, S. E. Zebiak and M. A. Cane, 1988: A model of the tropical Pacific sea surface temperature climatology. *J. Geophys. Res.*, **93,** 1265–1280.

Weare, B. C., P. T. Strub and M. D. Samuel, 1980: *Marine Climate Atlas of the Tropical Pacific Ocean.* Dept. of Land, Air and Water Resources, University of California, Davis, 147 pp.

——, —— and ——, 1981: Annual mean surface heat fluxes in the tropical Pacific Ocean. *J. Phys. Oceanogr.*, **11,** 705–717.

Zebiak, S. E., and M. A. Cane, 1987: A model El Niño southern oscillation. *Mon. Wea. Rev.*, **115,** 2262–2278.